*River, Coastal and Estuarine Morphodynamics: RCEM2011*


# Velocity of the particles entrained by a turbulent flow above an erodible bed composed of a mixture of two grains sizes

Morgane HOUSSAIS, Eric LAJEUNESSE, Olivier DEVAUCHELLE
*Equipe de dynamique des fluides géologiques*
*Institut de Physique du Globe de Paris, Sorbonne Paris Cité, Université Paris Diderot, UMR 7154 CNRS, F-75005 Paris, France*

ABSTRACT: We report the results of an experimental investigation of bimodal bedload transport. The experiments are carried out in a tilted rectangular flume, partially filled with an erodible bed composed of a mixture of quartz grains of two different sizes (0.7 and 2.2 mm) sheared by a steady and spatially uniform turbulent flow. A high-speed video imaging system allows us to study the trajectories of the particles of both sizes. Here we discuss the influence of the sediment bed granulometry on the velocities of the large particles ($D$ = 2.2 mm). The analysis of the experimental results shows that the PDFs of the streamwise velocity component of the large particles follow a Gaussian law. This is different from the exponential PDFs measured with the same sediments but in the case of a bed of uniform grain size (Lajeunesse *et al*., 2010). Despite this difference, the mean velocity of the large particles $V_2$ varies linearly with the shear velocity $u_*$, following a law similar to the one measured with the same sediments but in the case of a bed of uniform grain size.

## 1 INTRODUCTION

The wide range of grain sizes found in most rivers, especially gravel bed rivers, poses a difficult problem for the prediction of bedload transport rate. As stated by Wilcock and Kenworthy (2002), grain size influences sediment transport in two different ways. For given flow conditions above a bed of homogeneous sediments, transport is controlled by the absolute size of sediments, small grains being more mobile than large ones. However, when the sediment bed is a mixture of different grain sizes, relative size effects tend to increase the transport rate of larger grains and decrease the transport rate of smaller grains (Wilcock, 1993, 2001, Wilcock and Kenworthy 2002). This effect is very sensitive to the composition of the mixture which can change during transport and in response to variations in flow and sediment supply. Relative size effects influence the transport rate of each individual size and, consequently, the overall transport rate in a gravel bed river (Kunhle and Southard, 1988; Wilcock and Crowe, 2003; Parker, 2006). They also control important fluvial processes such as patches formation (Nelson *et al*, 2010) or downstream fining (Paola *et al*., 1992; Paola and Seal, 1995). However the relationship between bed coverage, transport rate and bed shear stress is still poorly understood (Wren *et al*., 2011).

Determining how granulometry influences sediment transport has been the goal of a large number of studies. A first approach consists in avoiding part of the difficulties associated with specifying individual size distribution by predicting the total transport rate as a function of a single representative grain size, usually the median diameter $D_{50}$ of the grain size distribution (Peter-Meyer and Müller, 1948). Within the frame of this approach, the volumetric transport rate per unit river width $q_s$ is related to the flow shear stress $\tau$ by the Peter-Meyer and Müller (1948) equation:

$$q_s^* = \alpha \cdot (\tau^* - \tau_c^*)^{3/2} \tag{1}$$

where α is a dimensionless coefficient, $q_s^*$ is a dimensionless transport rate called the Einstein number and $\tau^*$ is a dimensionless shear stress called the Shields number:

$$q_s^* = \frac{q_s}{\sqrt{RgD_{50}^3}} \qquad \tau^* = \frac{\tau}{\rho RgD_{50}} \qquad R = \frac{\rho_s - \rho}{\rho} \tag{2}$$

where $g$ is the gravitational acceleration, $\rho$ and $\rho_s$ are the fluid and sediment densities. The critical Shields number $\tau_c^*$ is the value of $\tau^*$ below which sediment transport cancels (Meyer-Peter and Müller, 1948; Shields, 1936). This approach is practical because the only sediment information required is the representative size. It is however unable to predict changes in grain size and it is also likely to underpredict the transport rate of finer fractions which may be much larger than that of the coarser fractions (Leopold, 1992; Lisle, 1995).

A second approach consists in discretizing the grain size distribution into a finite number $N$ of fractions of characteristic size $D_i$. The transport rate $q_{s,i}$ of each fraction $i$ is then modeled by a generalized form of the Meyer-Peter and Müller equation (Wilcock, 1988; Parker, 2006):

$$\frac{q_{s,i}^*}{\Phi_i} = \beta \cdot (\tau_i^* - \kappa \cdot \tau_{c,i}^*)^{\varepsilon} \qquad \text{for } i = 1,2, \ldots, N \tag{3}$$

where:

$$q_{s,i}^* = \frac{q_s}{\sqrt{RgD_i^3}} \qquad q_s^* = \sum_i q_{s,i}^* \qquad \tau_i^* = \frac{\tau}{\rho RgD_i} \tag{4}$$

and $\Phi_i$ is the fraction of the surface of the bed covered with grains of size $D_i$; $\kappa$, $\varepsilon$, $\beta$ and $\tau^*_c$ are empirical functions of the grain size distribution determined from flume experiments (Parker *et al*., 1982; Kuhnle and Southard,1988; Wilcock, 1998; Parker, 2006). $\tau^*_c$, for example, is usually related to the ratio $D_i/D_c$, $D_c$ being a characteristic size of the bed distribution, generally the $D_{50}$ or the $D_{84}$.

The transport laws discussed so far rely on the fit of sediment transport rate curves established from flume experiments with two shortcomings. First, the physical signification of the coefficients involved in equation (3) is unclear. Secondly, these transport laws establish a relation between the local flow rate of particles and the local shear stress exerted by the fluid flow on the bed. These relations consider implicitly that the particle flux is in equilibrium with the shear stress, so that their use in non-equilibrium conditions, i.e., when the shear stress varies in space or time, is questionable (Charru and Hinch, 2006; Lajeunesse *et al*., 2010; Devauchelle *et al*., 2010; 2010b).

An alternative way to consider the problem of bedload transport is to decompose the transport rate as the product of $n_i$, the number of moving particles of size $D_i$ per unit bed area, times their average velocity $V_i$:

$$q_{s,i} = \delta_i \cdot n_i \cdot V_i \tag{5}$$

where $\delta_i$ is the volume of an individual particle of size $D_i$. A better insight into the problem of bedload transport can indeed be gained from separate measurements of $n_i$ and $V_i$ as demonstrated by Lajeunesse *et al*. (2010) in the case of sediments of homogenous size. Following this approach, we present here the preliminary results of an experimental investigation of bedload transport above a sediment bed composed of quartz grains of two different sizes ($D_1$ =0.7 and $D_2$ =2.2 mm) sheared by a steady and spatially uniform turbulent flow. Here, we focus on the velocity of the coarse particles, $V_2$, and how it is influenced by the proportion of fine sediments.

## 2 EXPERIMENTAL PROCEDURE

### 2.1 *Experimental Setup*

The experiments were conducted in a tilted 9.6 cm wide laboratory flume with a working length of 240 cm (Figure 1a). The bottom of the flume was covered with a sediment bed composed of a mixture of small (average size $D_1$=0.7 mm and standard deviation 0.1 mm) and large (average size $D_2$=2.2 mm and standard deviation 0.4 mm) quartz grains of density $\rho_s$=2650 kg.m$^3$. Both grain populations follow a Gaussian size distribution.

The bed, typically 10 centimeters thick, was flattened by sweeping a rake, which tilt and height was constrained by two rails parallel to the channel. The bed slope S was measured with a digital inclinometer

(accuracy 0.1 ϑ). Once the bed was ready, water was injected by a pump at the upstream flume inlet with a constant flow discharge per unit width $Q_w$ measured with a flow-meter (accuracy 0.01 L/minute). To prevent any disturbance of the bed, water was not injected as a point source but rather it overflowed smoothly onto the river bed via a small reservoir (see Figure 1a). The reservoir extended across the full width of the channel and therefore guaranteed a flow injection that was uniform across the channel width. In all experimental runs the discharge was high enough for the flow to form across the full width of the flume.

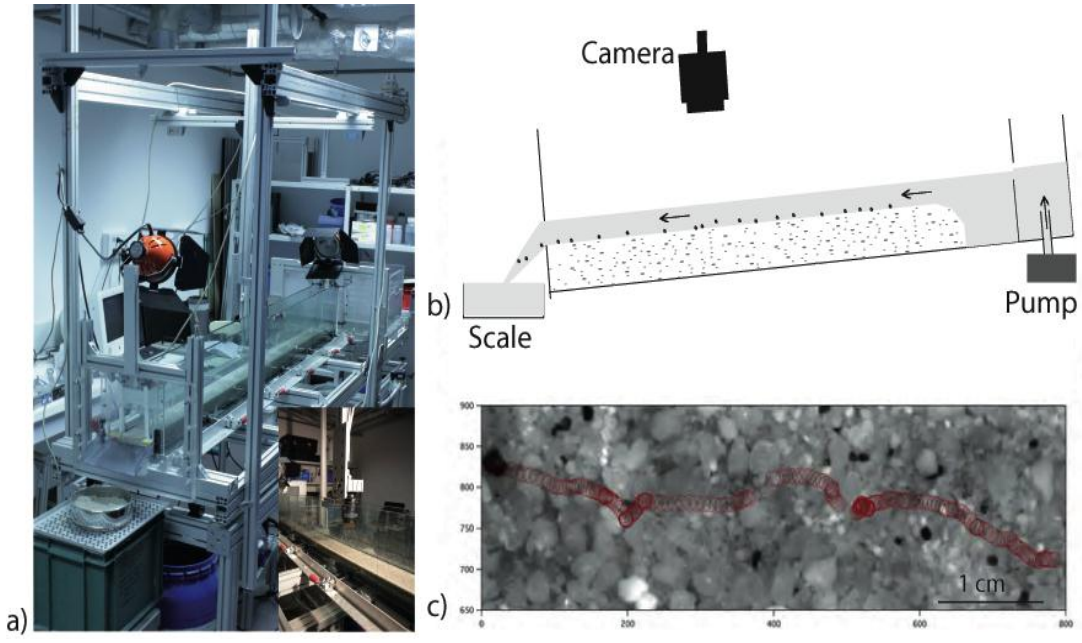


Figure 1 a) Pictures and b) sketch of the experimental setup; c) trajectory of a coarse grain recorded with the fast camera ($\tau^*_2$ = 0.035, $H/D_2$ = 6.25, $S$ = 0.012, $Re_s$ = 426.5 and $\Phi_2$= 32%)

Sediment particles transported by the flow settled out in a constant water level overflow tank located at the flume outlet. The tank rested on a high-precision scale (accuracy 0.1 g) connected to a computer that recorded the weight every 5 s. The total sediment discharge per unit river width $q_s$ was deduced from the sediment cumulative mass. The initiation of the flow was followed by a transient phase which lasted for about two minutes. After this transient, the transport rate reached a steady state. All the experimental measurements described hereafter were performed during this steady state regime and as long as the bed was flat.

Our setup provides real time measurements of the total sediment rate only. The fractional transport rates for each grain size, $q_{s1}$ and $q_{s2}$, were estimated by interposing a grid between the flume outlet and the overflowing tank once the steady state regime had been reached. $q_{s1}$ and $q_{s2}$ were then estimated by sieving and weighting the sediments accumulated over the grid.

Because we did not feed sediment at the river inlet, an erosion wave slowly propagated from the inlet towards the outlet of the flume. All our experiments were stopped well before this degradation wave had reached the middle of the flume where we performed our measurements so that it never interfered with our results. Indeed the slope of the river bed measured at the end of each experimental run was equal to the initial slope within the experimental accuracy.

The water flow depth $H$ measured with a ruler (accuracy ± 1 mm) on three locations regularly spaced along the flume was constant along the section of the flume (within the experimental accuracy). The flow was therefore uniform. In these conditions, the shear stress on the sediment bed and the shear velocity were estimated using the classical steady flow assumption

$$u^* = \sqrt{\frac{\tau}{\rho}} = \sqrt{gHS} \quad , \qquad \tau = \rho g H S \tag{6}$$

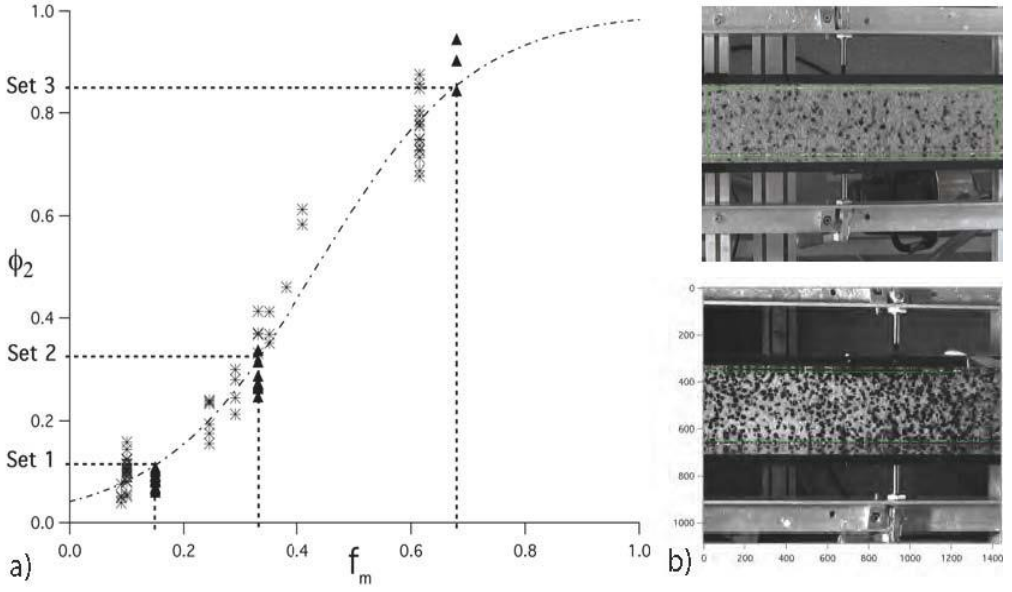


Figure 2 a) Surface fraction of the bed covered with coarse grains $\Phi_2$ as a function of the mass fraction of coarse grains in the mixture $f_m$. Stars: $\Phi_2$ values calculated from automatic image analysis, triangles: $\Phi_2$ values measured by direct counting of the coarse grains. The dashed line corresponds to a fit of the data by a sigmoid function. b) Views of the sediment bed with $\Phi_2 = 0.1$ (upper image) and $\Phi_2 = 0.21$ (lower image). All the coarse grains are dyed in black for both pictures

The Shields number for each grain size *i* is then given by :

$$\tau_i^* = \frac{HS}{RD_i} \quad . \tag{7}$$

The accuracy on $\tau$ and $\tau_i^*$ results from the uncertainties on the measurements on *H* and *S*.

The fraction of the surface of the bed covered with coarse grains $\Phi_2$ is an important parameter which needs to be estimated for each experimental run. This was achieved as follows. First, we performed a series of specific runs, for which all the coarse grains were dyed in black. Photos of the bed taken at the beginning and at the end of each experiment were processed to compute the surface of the image covered by the coarse grains. Dyeing the whole coarse grains population facilitates the measurement of $\Phi_2$. It is however a source of errors for the measurement of the particle velocity. This is why we performed a second series of experiments where $\Phi_2$ was measured from a direct counting of the coarse grains within the field of view. The values of $\Phi_2$ deduced from the two methods are plotted on Figure 2 as a function of the mass fraction of coarse grains in the mixture $f_m$. Both methods produce comparable results. Moreover, the values of $\Phi_2$ collapse on a curve which can be approximated by a sigmoid function of $f_m$:

$$\Phi_2 = \frac{1}{1+e^{(0.44-f_m)/0.14}} \tag{8}$$

Therefore, $\Phi_2$ was computed for each experimental run by inverting equation (8).

2.2 *Data analysis*

For each experimental run, we measured the instantaneous velocities of the coarse grains. This was achieved by dyeing in black a fraction of the coarse grains so that their trajectories could be tracked by processing the images acquired with a high-speed camera (250 images/s). The spatial resolution of the images was such that the particle diameter was about 50 pixels and the size of the field of view of the order of 20×20 particle diameters. Under these conditions, we were able to determine the position of the center of mass of a particle on an image with a precision of 0.5 mm. However the oscillations of the water surface, which are the main source of experimental error, degraded the accuracy of these measurements

causing an apparent movement of particles at rest. The corresponding false velocities were calibrated for each experimental run by computing this apparent velocity. This allowed us to define a cutoff velocity in the range 1–3 cm s−1, depending on the water flow rate, below which the particle was considered to be at rest (i.e., the velocity measurement was not taken into account).

Finally, the number of coarse moving particles per unit area of the bed $n_2$ were also measured for each experimental run by counting the total number of coarse particles (whether dyed or not) moving between two successive frames within the field of view, and averaging over a sufficiently large number of frames for the mean to converge.

## 3 RESULTS AND DISCUSSIONS

We performed two series of experiments corresponding to respectively $\Phi_2 = 0.11$ and $\Phi_2 = 0.32$. For each series of experiments, runs were performed with bed slopes ranging from $4.5.10^{-3}$ to $3.2.10^{-2}$ and water discharges ranging from 10 to 30 L $min^{-1}$. The corresponding range of $\tau_2^*$ is $1.75.10^{-3}$ to $9.6.10^{-2}$.

The instantaneous values of $V_{x,2}$, the streamwise velocity component of the large dyed particles in motion, were measured for each experimental run as described in section 2. Several thousands of velocity measurements were thus performed for each experiment, allowing us to estimate experimentally the probability density functions (PDF) of $V_{x,2}$, samples of which are shown in Figure 3. For the explored range of parameters, the PDFs of $V_{x,2}$, are well fitted by a Gaussian law (Figure 3). They are therefore different from the exponential particle velocity PDFs measured for unimodal sediment transport (i.e. $\Phi_2$=1) (Lajeunesse *et al*., 2010). This difference suggests that the shape of the trajectories of the large grains is affected by the presence of a relatively large proportion of smaller grains. We believe that the presence of small grains surrounding the large grains favor saltation at the expense of rolling. This is however only a conjecture and more experimental work is needed to support that idea.

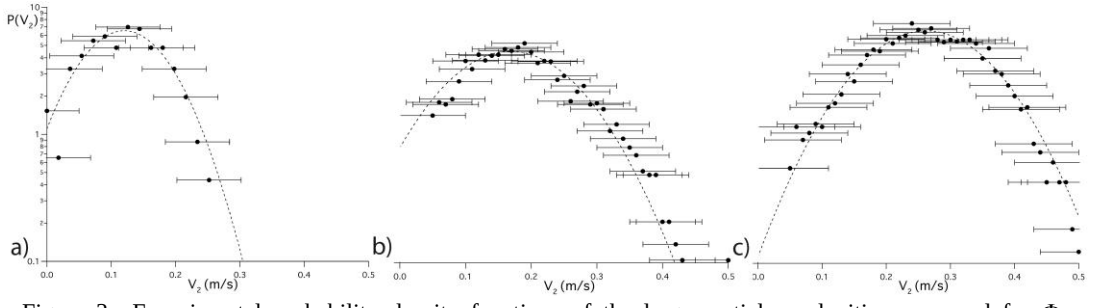


Figure 3 Experimental probability density functions of the large particles velocities measured for $\Phi_2$= 0.11 (experimental series 1) and a) $\tau^*_2 = 0.032$, b) $\tau^*_2 = 0.062$ and c) $\tau^*_2 = 0.096$. Dashed lines are best Gaussian fits

For each experimental run, the mean velocity of the large particles $V_2$ was computed from a Gaussian fit of the PDF of $V_{x,2}$. The values of $V_2$ are plotted as a function of $u_*$ on Figure 4 together with the data obtained with the same sediment but in the case of a bed of uniform grain size ($\Phi_2 = 1$). For each experimental series, $V_2$ varies linearly with $u_*$, as already observed for a bed of uniform grain size (Lajeunesse *et al*., 2010). Moreover, for a given shear velocity $u_*$, the mean particle velocity $V_2$ increases with the proportion of small particles, i.e. when $\Phi_2$ decreases.

A fit of the data by the function $a\,(u_* - \gamma)$ leads to the values of the coefficients reported in Table 1. The increase of $\gamma$ with $\Phi_2$ most likely reflects the decrease of the critical Shields number when the proportion of the fine particles increases.

Table 1 Results of the best linear fits of the coarse particles velocities from the 3 series

| **Series** | $\boldsymbol{\Phi_2}$ | $\boldsymbol{a}$ | $\boldsymbol{\gamma}$ (m/s) |
|---|---|---|---|
| 1 | 0.11 | 5.6 ±0.44 | 0.014 ±0.002 |
| 2 | 0.32 | 4.6 ±0.33 | 0.015 ±0.002 |
| Homogeneous | 1 | 4.4 ±0.2 | 0.031 ±0.004 |

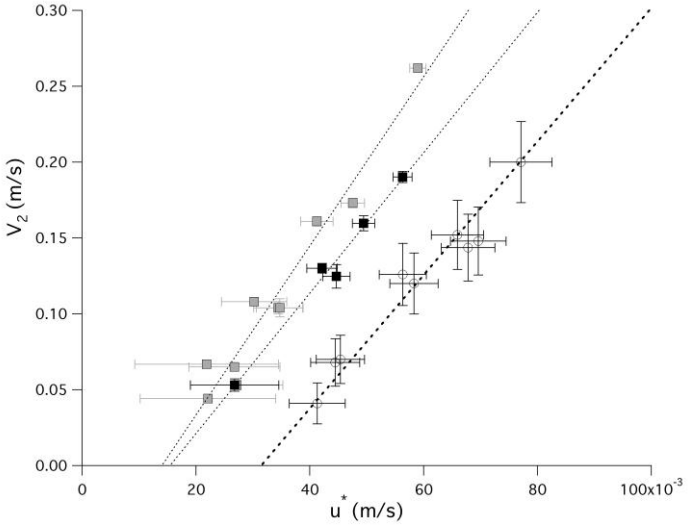


Figure 4 Mean velocity of the large particles $V_2$ as a function of $u_*$. Grey and black squares correspond to the experimental series 1 ($\Phi_2 = 0.11$) and 2 ($\Phi_2 = 0.32$). The circles correspond to the mean velocities measured with the same sediment but in the case of a bed of uniform grain size ($\Phi_2 = 1$) by Lajeunesse *et al*. (2010). Dashed lines are best linear fits

## 4 CONCLUSIONS

We have reported the preliminary results of an experimental investigation of bedload transport above an erodible bed composed of grains of two different sizes (0.7 and 2.2 mm) sheared by a steady and spatially uniform turbulent flow. Using a high-speed video imaging system, we tracked the trajectories of the large particles. The analysis of the experimental results leads to two important results :

1. The PDFs of the streamwise velocity component of the large particles follow a Gaussian law. This is different from the exponential PDFs measured with the same sediments but in the case of a bed of uniform grain size ($\Phi_2 = 1$) (Lajeunesse *et al*., 2010).
2. The mean velocity of the large particles $V_2$ varies linearly with $u^*$ as already observed in the case of a bed of uniform grain size (Lajeunesse *et al*., 2010).

We are currently pursuing this investigation by studying how the velocity distribution of the fine sediments, the threshold Shield stresses and the surface density of moving particles vary with the grain size distribution.

## 5 ACKNOWLEDGEMENTS

The research program was funded by ANR-09-RISK-004/GESTRANS grant.
This is IPGP contribution N °3169.

## REFERENCES

Charru F., and Hinch E. 2006, Ripple formation on a particle bed sheared by a viscous liquid. Part 1. Steady flow, J. Fluid Mech., 550, 111–121.

Devauchelle O., Malverti L., Lajeunesse É., Josserand C., Lagrée P.-Y., and Métivier F. 2010, Rhomboid beach pattern: A laboratory investigation, J. Geophys. Res., 115, F02017, doi:10.1029/2009JF001471.

Kuhnle R. A., and Southard J. B. 1988, Bed load transport fluctuations in a gravel bed laboratory channel, Water Resour. Res., 24(2), 247–260, doi:10.1029/WR024i002p00247.

Lajeunesse E., Malverti L. & Charru F. 2010, Bedload transport in turbulent flow at the grain scale: experiments and modeling, J. Geophys. Res., 115, F04001, doi:10.1029/2009JF001628.

Lisle T. E. 1995, Particle size variations between bed load and bed material in natural gravel bed channels,Water Resour. Res., 31(4), 1107– 1118.

Leopold L. B. 1992, Sediment size that determines channel morphology, in Dynamics of Gravel-Bed Rivers, edited by P. Billi et al., pp. 297–307, John Wiley, New York.

Meyer-Peter E., and Müller R. 1948, Formulas for bed-load transport, paper presented at 2nd Meeting of International Association for Hydraulic Research, Int. Assoc. for Hydraul. Res., Stockholm.
Nelson P. A., Dietrich W. E., and Venditti J. G. 2010, Bed topography and the development of forced bed surface patches, J. Geophys. Res., 115, F04024, doi:10.1029/2010JF001747.
Paola C., Hellert P., and Angevine C. 1992, The large-scale dynamics of grain-size variation in alluvial basins, 1 : theory, Basin Research, 4, 73–90.
Paola C., and Seal R. 1995, Grain Size Patchiness as a Cause of Selective Deposition and Downstream Fining, Water Resour. Res., 31(5), 1395–1407, doi:10.1029/94WR02975.
Parker G., Klingeman P. C., and McLean D. L 1982b, Bedload and size distribution in paved gravel-bed streams, J. Hydraul. Div. Am. Soc. Civ. Eng., 108(HY4), 544–571.
Parker G. 2006, Sedimentation Engineering (Manuals and Reports on Engineering Practice No.54), chap. 3, American Society of Civil Engineers.
Shields I. 1936, Anwendung der ahnlichkeitmechanik und der turbulenzforschung auf die gescheibebewegung, Mitt. Preuss Vers. Wasserbau Schiffbau, 26, 5–24.
Wilcock, P. R. 1988, Methods for estimating the critical shear stress of individual fractions in mixed-size sediment, Water Resour. Res., 24(7), 1127– 1135.
Wilcock P. R. 1998, Critical shear stress of natural sediments, J. Hydraul. Eng., 119, 491–505, 1993. Wilcock, P. R., Two-fraction model of initial sediment motion in gravel-bed rivers, Science, 280, 410–412.
Wilcock P. R. 2001, Toward a practical method for estimating sediment transport rates in gravel-bed rivers, Earth Surf. Processes Landforms, 27, 1395– 1408.
Wilcock P. R., and Kenworthy S. T. 2002, A two-fraction model for the transport of sand/gravel mixtures, Water Resour. Res., 38(10), 1194, doi:10.1029/2001WR000684.
Wilcock P.R, and Crowe, J.C. 2003, Surface-based transport model for mixed-size sediment, J. of Hydraulic Engineering, pp. 120-128.
Wren D. G., Langendoen E. J., and Kuhnle R. A. 2011, Effects of sand addition on turbulent flow over an immobile gravel bed, J. Geophys. Res., 116, F01018, doi:10.1029/2010JF001859.